

**The narrow-bandgap photothermal material based on donor-acceptor structure
for the solar-thermal conversion application**

Ruoyu Zhang,^a Nanxi Jin,^b Tao Jia*^a, Luoqing Wang,^a Jing Liu,^a Mengmeng Nan,^a Shuo Qi,^a Siqu Liu,^a
and Yuyu Pan*^c

- ^a Key Laboratory of Forest Plant Ecology, Ministry of Education, Engineering Research Center of Forest Bio-Preparation, Heilongjiang Provincial Key Laboratory of Ecological Utilization of Forestry Based Active Substances, College of Chemistry, Chemical Engineering and Resource Utilization, Northeast Forestry University, 26 Hexing Road, Harbin 150040, P. R. China.
- ^b Sungkyunkwan University, Seoul City, Korea.
- ^c School of Petrochemical Engineering, Shenyang University of Technology, 30 Guanghua Street, Liaoyang, 111003, P. R. China

Reagents and materials

All solvents and reagents are purchased from J&K Scientific Ltd. Co and Derthon Optoelectronic Materials Science Technology Co., Ltd. for direct use.

Synthesis of 4,8-bis(3-(2-ethylhexyl)-[2,2'-bithiophen]-5-yl)benzo[1,2-c:4,5-c']bis([1,2,5]thiadiazole) (2TP-BBT)

4,8-bis(5-bromo-4-(2-ethylhexyl)thiophen-2-yl)benzo[1,2-c:4,5-c']bis[1,2,5]thiadiazole (2.3 g, 3.1 mmol), trimethyl-2-thienyl-Stannane (1.7 g, 6.9 mmol), Pd[PPh₃]₂Cl₂ (0.2 g), and THF (40 mL) was added into a round bottom 100 mL Schlenck flask. The mixture was stirred at 80 °C and refluxed again under N₂ for 24 h. The mixture was cooled down to room temperature and poured into methanol (150 mL). The crude product was purified further by column chromatography (silica gel, hexane/toluene (4:1, v/v)) to give dark green solid. (1.5 g). Yield: 60%. ¹H NMR (500 MHz, Chloroform-d) δ 8.84 (s, 1H), 7.39 (dd, J = 5.1, 1.1 Hz, 1H), 7.36 (dd, J = 3.6, 1.1 Hz, 1H), 7.27 (s, 2H), 7.13 (dd, J = 5.1, 3.6 Hz, 1H), 2.87 (d, J = 7.3 Hz, 2H), 1.83 (p, J = 6.5 Hz, 1H), 1.50 – 1.30 (m, 4H), 1.30 (s, 6H), 1.32 – 1.24 (m, 1H), 0.89 (dt, J = 16.5, 7.3 Hz, 6H). ESI-MS (M): m/z: 746.94 [M]⁺ (calcd:748.19).

General information

¹H NMR spectra were measured on Zhongke-Niujiu Quantum-I 400 MHz with tetramethylsilane (TMS) as the internal standard. Mass spectra was recorded on a Thermo Fisher ITQ1100 GC/MS mass spectrometer. The UV-vis-NIR vis absorption spectra of 2TP-BBT in solvent and solid powder were recorded by the Shimadzu UV-2550 spectrophotometer and Analytik Jena Specord 210 spectrophotometer equipped with an integrating sphere, respectively. The fluorescence spectra and absolute fluorescence quantum yield taken at room temperature were carried out on Edinburgh FLS920 steady state fluorimeter. Thermogravimetric analyse (TGA) was performed on a TA Q500 thermogravimeter by measuring their weight loss while heating at a rate of 10 K min⁻¹ from 40 to 800 °C under nitrogen.

Theoretical calculation

The density functional theory (DFT) calculations were operated using Gaussian 09 program package with the B3LYP/6-31g(d) method. The ground state geometries of

gas state were fully optimized by B3LYP method including Grimme's dispersion correction with 6-31G(d,p) basis set using Gaussian 09 software package. HOMO and LUMO were visualized with Gaussview 5.0. We calculated the reorganization energy (λ) using the DUSHIN program.

Photothermal experiments

SEM (EM-30plus) was used to observe the morphology of non-woven fabric. Infrared thermal imager (TESTO-869) was used to record the change of temperature. The experiments of water evaporation and thermoelectric generation were carried out with xenon Cell-S500/350 light source (AM 1.5 G spectral filter). TEC1-12706 was used as thermoelectric device, and the open-circuit voltage data was obtained by FLUKE 8846A system. The 980 nm laser (MW-GX-980/5000 mW) is produced by Changchun New Industries Optoelectronics Tech. Co., Ltd, China.

Calculation of the photothermal conversion efficiency

The conversion efficiency was determined according to previous method. Details are as follows: Based on the total energy balance for this system:

$$\sum_i m_i C_{p,i} \frac{dT}{dt} = Q_s - Q_{loss}$$

where m_i (0.3263 g) and $C_{p,i}$ (0.8 J (g °C)⁻¹) are the mass and heat capacity of system components (2TP-BBT samples and quartz glass), respectively. Q_s is the photothermal heat energy inputted by irradiating NIR laser to 2TP-BBT samples, and Q_{loss} is thermal energy lost to the surroundings. When the temperature is maximum, the system is in balance.

$$Q_s = Q_{loss} = hS\Delta T_{max}$$

where h is heat transfer coefficient, S is the surface area of the container, ΔT_{max} is the maximum temperature change. The photothermal conversion efficiency η is calculated from the following equation:

$$\eta = \frac{hS\Delta T_{max}}{I(1 - 10^{-A_{980}})}$$

where I is the laser power (0.8 W cm⁻²) and A_{980} is the absorbance of the samples at the wavelength of 980 nm (1.272).

In order to obtain the hS , a dimensionless driving force temperature, θ is introduced as follows:

$$\theta = \frac{T - T_{surr}}{T_{max} - T_{surr}}$$

where T is the temperature of 2TP-BBT, T_{max} is the maximum system temperature (117 °C), and T_{surr} is the initial temperature (23 °C).

The sample system time constant τ_s

$$\tau_s = \frac{\sum_i m_i C_{p,i}}{hS}$$

thus
$$\frac{d\theta}{dt} = \frac{1}{\tau_s} \frac{Q_s}{hS\Delta T_{max}} - \frac{\theta}{\tau_s}$$

when the laser is off, $Q_s = 0$, therefore
$$\frac{d\theta}{dt} = -\frac{\theta}{\tau_s}$$
, and $t = -\tau_s \ln \theta$

so hS could be calculated from the slope of cooling time vs $\ln \theta$. Therefore, τ_s is 74.7 s (Figure S6) and the photothermal conversion efficiency η is 43.32%.

Calculation of the photothermal conversion efficiency

The 1 mg 2TP-BBT powder was dispersed in 1 mL water with an insulating layer and illuminating the solution with simulated solar light. The temperature of the solution was recorded using a thermal imaging camera upon simulated solar light irradiation for 20 min and energy conversion efficiency (η) was calculated as the following formula :

$$\eta = \frac{Q}{E} = \frac{Q_1 - Q_2}{E}$$

Where Q refers to the thermal energy generated (i.e., $Q = Q_1 - Q_2$), Q_1 is the thermal energy generated of 2TP-BBT and Q_2 is the thermal energy generated of pure water. E refers to the total energy of the incident light. Q is determined by the heat capacity (C), density (ρ), volume (V) and ΔT over the period of irradiation of the solution; E is determined by the power (P) of the incident light, the irradiation area (S) and irradiation time (t). Therefore, the specific formula is as follows:

$$Q_1 = Cm\Delta T_1 = C\rho V\Delta T_1$$

$$Q_2 = Cm\Delta T_2 = C\rho V\Delta T_2$$

$$E = PSt$$

In this paper, Since samples are present in very low amounts in the solution, values of C ($4.2 \text{ J g}^{-1} \text{ }^\circ\text{C}^{-1}$) and ρ (1 g cm^{-3}) for water were used in the calculations.

For example, the surface temperature of 2TP-BBT micelles was $45.0 \text{ }^\circ\text{C}$ during the irradiation process, and the initial temperature is $18.2 \text{ }^\circ\text{C}$, therefore ΔT is $26.8 \text{ }^\circ\text{C}$. As the above fomulas,

$$Q_1 = C\rho V\Delta T_1 = 4.2 \times 1 \times 1 \times (45.0 - 18.2) = 112.98 \text{ J}$$

$$Q_2 = C\rho V\Delta T_2 = 4.2 \times 1 \times 1 \times (36.0 - 20.7) = 64.26 \text{ J}$$

$$E = PSt = 0.1 \times 1.8137 \times 1200 = 217.644 \text{ W} \cdot \text{s}$$

$$\eta = \frac{Q_1 - Q_2}{E} = 112.98 - 64.26 / 217.644 = 22.38\%$$

As a result, 2TP-BBT energy conversion efficiency $\eta = Q_1 - Q_2 / E = 22.38\%$ when the temperature difference is $26.8 \text{ }^\circ\text{C}$ is calculated.

Solar steam generation experiments

The load non-woven fabric rests on a small beaker that is filled with water. The sunlight, generated by a solar simulator with an optical filter for the standard AM 1.5 G spectrum (CEL-S500/350), irradiated at the sample under specific optical concentrations. The weight loss of water was measurement by an electronic mass balance and the temperature over the process was recorded by an IR thermal camera. The energy conversion efficiency was determined according to previous methods.

Desalination of seawater

Collected real seawater samples from the Yellow Sea in China for desalination. Inductively coupled plasma spectrometer (ICP-OES, Avio™ 200) was used to determine the concentration of four main ions (Na^+ , Mg^{2+} , Ca^{2+} , K^+) that originally existed in seawater before and after desalination.

Thermoelectric power generation

Commercial thermoelectric generator (TEC1-12706, long 40 mm, wide 40 mm, high 3.6 mm) was selected for power generation. The 2TP-BBT and silicon thermal conductive glue were evenly smeared on the upper surface of the thermoelectric sheet,

and the lower part was connected with the copper cold sheet. Thermoelectric open circuit voltage (VOC) were measured and recorded by FLUKE 8846A system electrometer instrument. The subsequent power generation was carried out on the 1.0, 2.0 and 5.0 kW m⁻² respectively, and the surface temperature was collected and recorded by infrared thermal imager.

Calculation of the efficiency for solar to vapor generation

The conversion efficiency η of solar energy in photothermal assisted water evaporation was calculated as the following formula.

$$\eta = \frac{\dot{m}h_{LV}}{C_{opt}P_0}$$

Where \dot{m} refers to the mass flux (evaporation rate) of water, h_{LV} refers to the total liquid vapor phase-change enthalpy (i.e., the sensible heat and the enthalpy of vaporization (i.e., $h_{LV} = Q + \Delta h_{vap}$)), Q is the energy provided to heat the system from the initial temperature to a final temperature, Δh_{vap} is the latent heat of vaporization of water P_0 is the nominal solar irradiation value of 1.0 kW m⁻², and C_{opt} represents the optical concentration. The schematic for the vaporization enthalpy of the vapor was as follows.

$$Q = C_{liquid} \times (T - T_0)$$

$$\Delta h_{vap} = Q_1 + \Delta h_{100} + Q_2$$

$$Q_1 = C_{liquid} \times (100 - T)$$

$$Q_2 = C_{vapor} \times (T - 100)$$

In this paper, C_{liquid} , the specific heat capacity of liquid water is a constant of 4.18 J (g °C)⁻¹. C_{vapor} , the specific heat capacity of water vapor is a constant of 1.865 J (g °C)⁻¹. Δh_{100} is the latent heat of vaporization of water at 100 °C, taken to be 2260 kJ kg⁻¹. The surface temperature of the 2TP-BBT/non-woven fabric was 41.0 °C during the evaporation process, therefore T is 41.0 °C. As the above formulas,

$$Q = C_{liquid} \times (T - T_0) = 4.18 \times (41.0 - 13.3) = 115.786 \text{ kJ kg}^{-1}$$

$$\begin{aligned} \Delta h_{vap} &= Q_1 + \Delta h_{100} + Q_2 = 4.18 \times (100 - 41.0) + 2260 + 1.865 \times (41.0 - 100) \\ &= 2396.585 \text{ kJ kg}^{-1} \end{aligned}$$

$$h_{LV} = Q + \Delta h_{vap} = 115.786 + 2396.585 = 2512.371 \text{ kJ kg}^{-1}$$

$$\dot{m} = 1.3512 \text{ kg m}^{-2} \text{ h}^{-1}$$

$$P_0 = 1000 \text{ W m}^{-2}$$

$$C_{opt} = 1$$

As a result, evaporation efficiency $\eta = \dot{m}h_{LV}/C_{opt}P_0 = 94.30\%$ when the latent heat of water vaporization at 41.0 °C (2500.056 kJ kg⁻¹) is used in calculation.

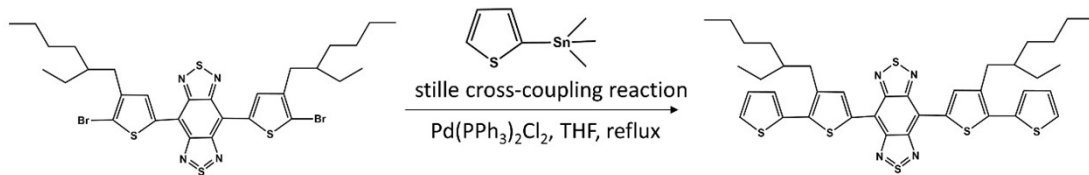
Calculation of the load efficiency of the 2TP-BBT on the non-woven fabric

The load efficiency η of 2TP-BBT on the non-woven fabric was calculated as the following formula:

$$\eta = \frac{m_1 - m_0}{m} = \frac{0.2178 - 0.2150}{0.0030} = 93.3\%$$

where m_1 is the mass of 2TP-BBT/non-woven fabric (0.2178 g), m_0 is the mass of blank non-woven fabric before impregnated (0.2150 g), and m is the mass of 2TP-BBT powder (0.0030 g). As a result, the load efficiency $\eta = 93.3\%$.

Supplementary figures and tables



Scheme S1. Synthetic routes of 2TP-BBT.

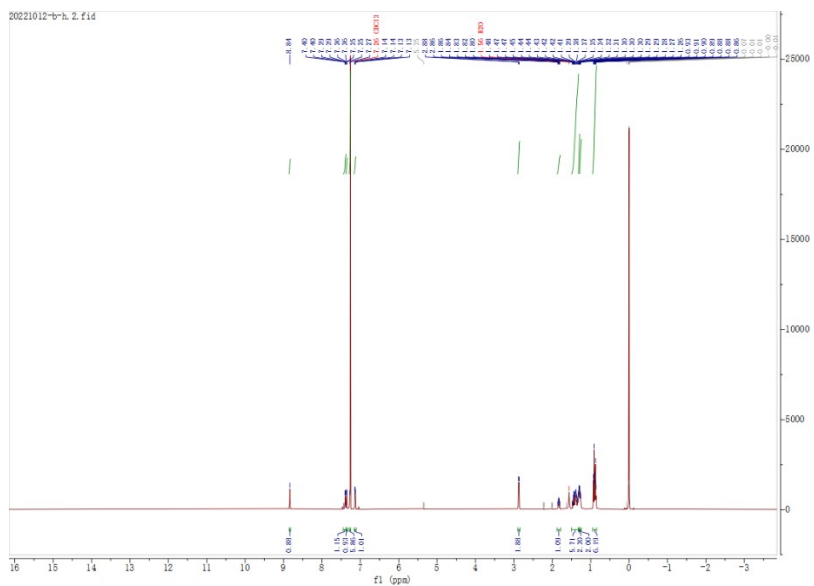


Figure S1. ^1H NMR spectrum of 2TP-BBT in Chloroform-d.

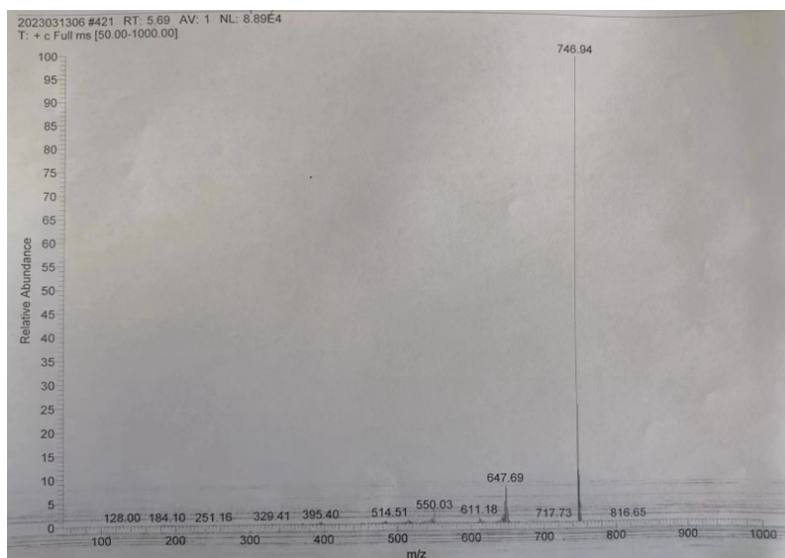


Figure S2. Mass spectrum of 2TP-BBT.

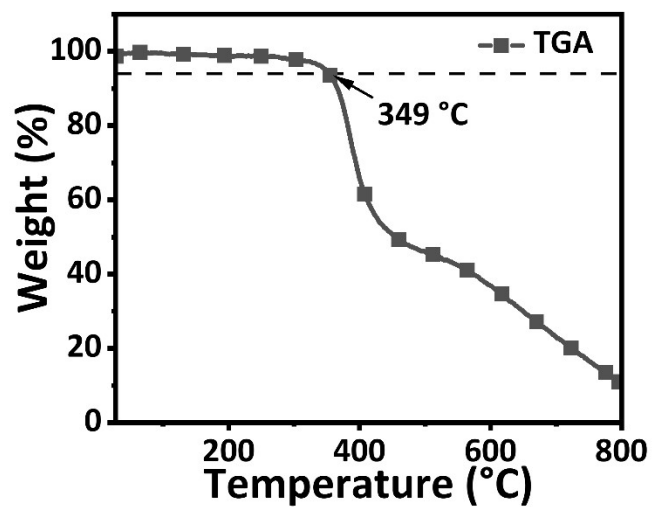


Figure S3. Thermogravimetric analysis curve of 2TP-BBT.

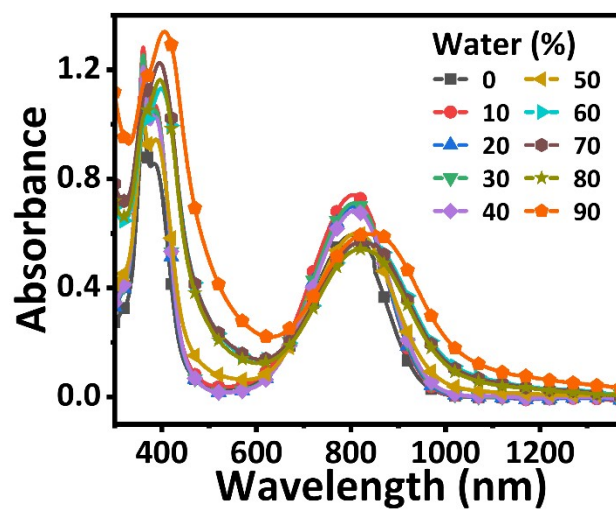


Figure S4. Absorption spectra of 2TP-BBT in tetrahydrofuran (THF) solutions with different water contents.

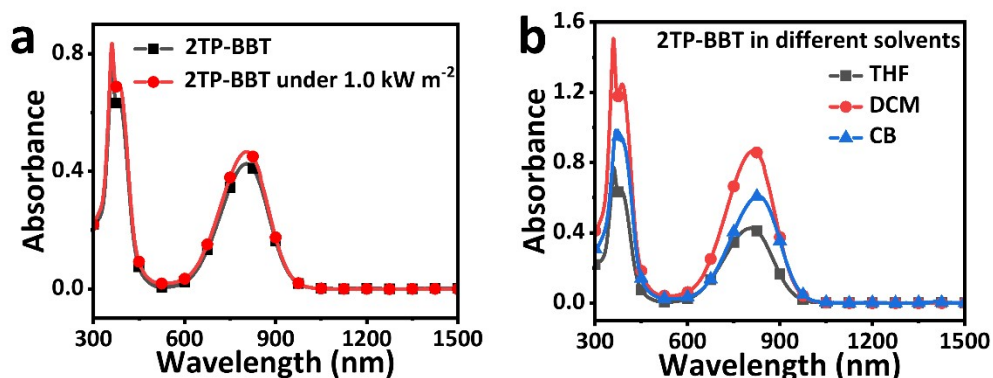


Figure S5. (a) Absorption spectra of 2TP-BBT in THF and 2TP-BBT (under 1.0 kW m⁻² for 2 h) in THF. (b) Absorption spectra of 2TP-BBT in different solvents (THF, Dichloromethane (DCM) and Chlorobenzene (CB), 20 μg mL⁻¹) at room temperature.

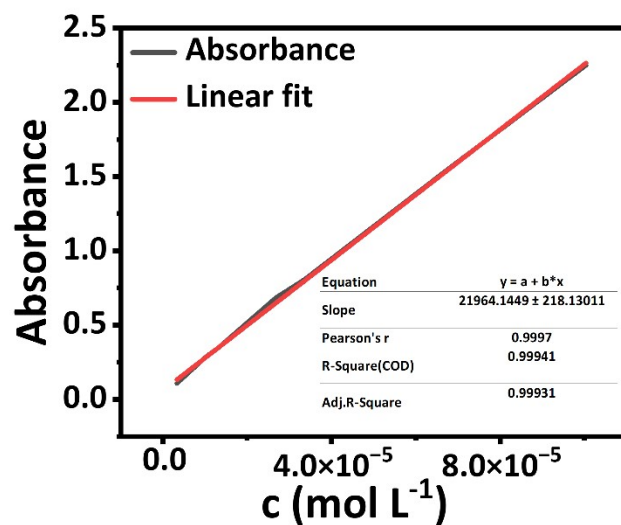


Figure S6. The absorption versus concentration curve of 2TP-BBT in THF.

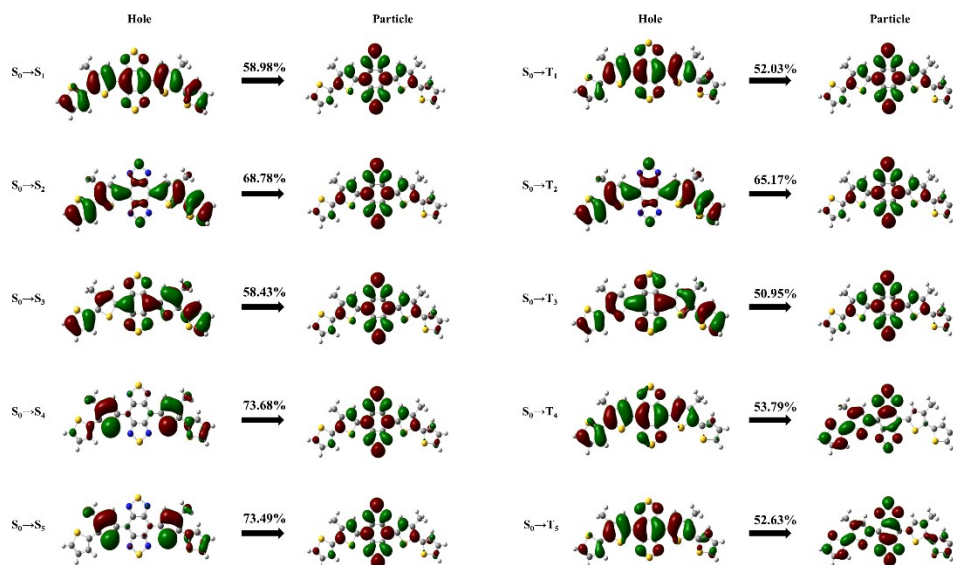


Figure S7. Optimized molecular structures.

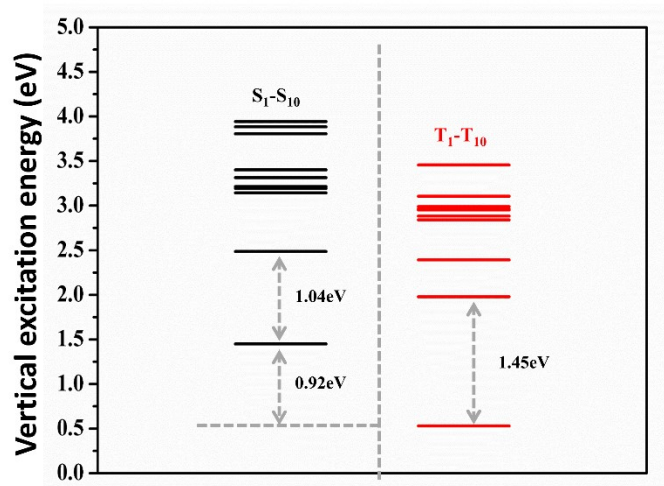


Figure S8. Energy-level diagram of 2TP-BBT.

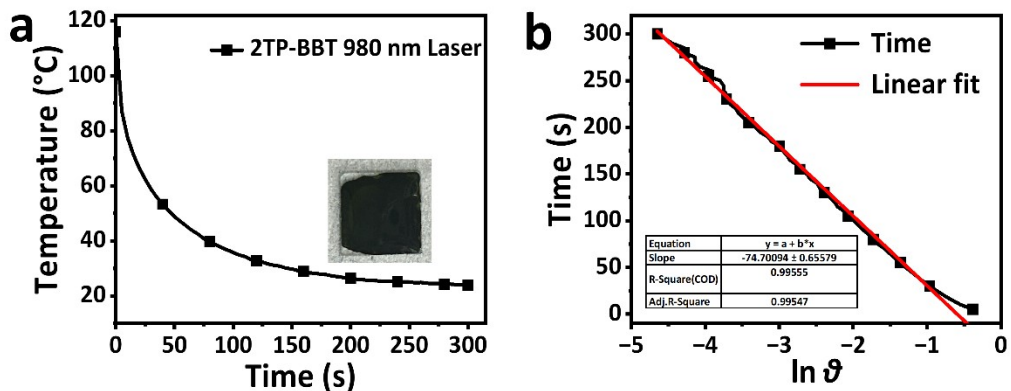


Figure S9. (a) Cooling curve of 2TP-BBT film after irradiation with 980 nm laser (0.8 W cm^{-2}) and (b) its corresponding time- $\ln\theta$ linear curve.

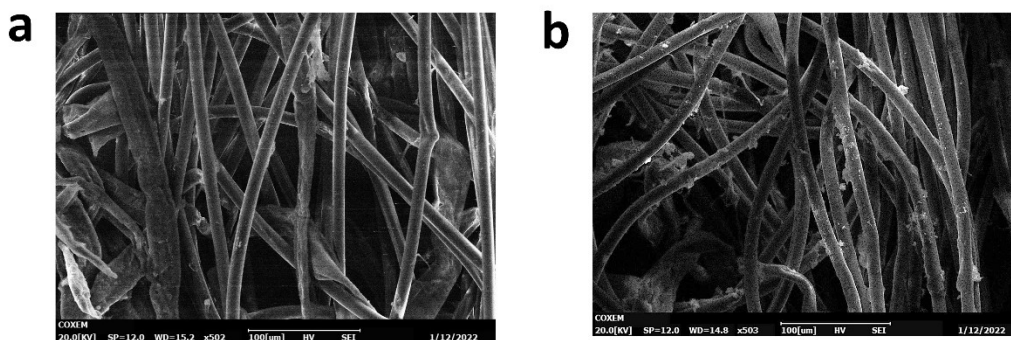


Figure S10. (a) Digital photos and SEM images of blank non-woven fabric and (b) 2TP-BBT/non-woven fabric.



Figure S11. 2TP-BBT/non-woven fabric change of load capacity before and after kneading and folding

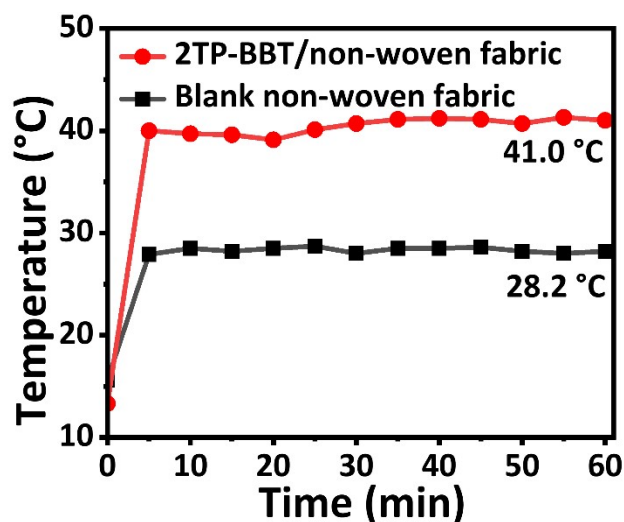


Figure S12. Temperature change over the course of one hour of water evaporation.

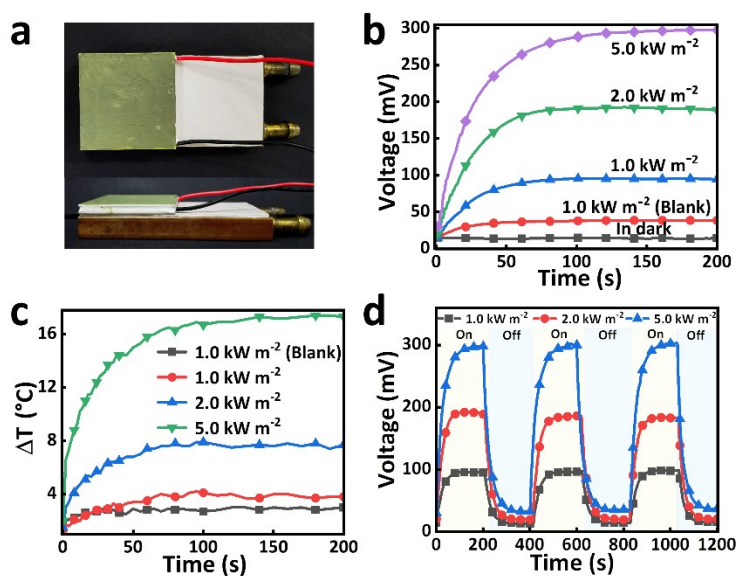


Figure S13. (a) Generating design of thermoelectric device. 2TP-BBT powder dosage is 10 mg. (b) Thermoelectric conversion capability of 2TP-BBT powder that is attached to the surface of the thermoelectric device under different solar intensities (dark, 1.0 kW m⁻² (Blank), 1.0 kW m⁻², 2.0 kW m⁻² and 5.0 kW m⁻²). (c) Temperature difference between the surface of a thermoelectric device and the circulating water under different solar intensity

(1.0 kW m⁻² (Blank), 1.0 kW m⁻², 2.0 kW m⁻² and 5.0 kW m⁻²). (d) Stabilizing thermoelectric generating property of 2TP-BBT powder during three cycles of on-off processes.

Supplementary Tables

Table S1

No.	Material name	Water evaporation rate (kg m ⁻² h ⁻¹)	Open-circuit voltage (mV)/Thermoelectric power generation
1	DDPA-PDN ¹	1.08	83
2	GDPA-QCN ²	1.30	90
3	DDHT ³	1.13	90
4	DCN-4CQA ⁴	0.97	92

Table S2

No.	Material name	Photothermal conversion efficiency (%)
1	GDPA-QCN ²	19
2	4OCSPC ⁵	17
3	DCN-4CQA ⁴	18
4	L-NPs ⁶	22
5	DDHT ³	13

References

1. Y. Cui, J. Liu, Z. Li, M. Ji, M. Zhao, M. Shen, X. Han, T. Jia, C. Li and Y. Wang, *Adv. Funct. Mater.*, 2021, **31**, 2106247.
2. J. Liu, Y. Cui, Y. Pan, Z. Chen, T. Jia, C. Li and Y. Wang, *Angew. Chem. Int. Ed.*, 2022, **61**, e202117087.
3. M. Zhao, Y. Zhu, Y. Pan, Y. Wang, T. Xu, X. Zhao, T. Jia, Z. Zhang and Z. Chen, *ACS Appl. Energy Mater.*, 2022, **5**, 15758-15767.
4. M. Shen, X. Zhao, L. Han, N. Jin, S. Liu, T. Jia, Z. Chen and X. Zhao, *Chemistry – A European Journal*, 2022, **28**, e202104137.
5. X. Han, Z. Wang, M. Shen, J. Liu, Y. Lei, Z. Li, T. Jia and Y. Wang, *J. Mater. Chem. A*, 2021, **9**, 24452-24459.
6. X. Zhao, C. Huang, D. Xiao, P. Wang, X. Luo, W. Liu, S. Liu, J. Li, S. Li and Z. Chen, *ACS Appl. Mater. Interfaces*, 2021, **13**, 7600-7607.